

Depolarization effect in liquid crystal displays

HAIWEI CHEN,¹ GUANJUN TAN,¹ MING-CHUN LI,² SEOK-LYUL LEE,² AND SHIN-TSON WU^{1,*}

¹College of Optics and Photonics, University of Central Florida, Orlando, Florida 32816, USA

²AU Optronics Corp., Hsinchu Science Park, Hsinchu 300, Taiwan

*swu@ucf.edu

Abstract: We develop a rigorous model to simulate an LCD's contrast ratio (CR) and viewing angle by considering the depolarization effect in thin-film transistor substrate, LC layer, color filter (CF) array, etc. To mitigate the depolarization effect, we propose a new device structure by adding a thin in-cell polarizer between LC layer and CF array. Based on the analysis using our new model, the maximum CR of a multi-domain vertical alignment (MVA) LCD can reach $> 20,000:1$, while for the fringe-field switching (FFS) mode it can reach $> 3000:1$. We also discuss other approaches to further enhance the CR. Our model is a powerful tool to analyze the CR degradation mechanism and to guide the future LCD device and material optimizations.

© 2017 Optical Society of America

OCIS codes: (160.3710) Liquid crystals; (230.3720) Liquid-crystal devices; (120.2040) Displays.

References and links

1. D. K. Yang and S. T. Wu, *Fundamentals of Liquid Crystal Devices*, 2nd Ed. (John Wiley & Sons, 2014).
2. H. Seetzen, W. Heidrich, W. Stuerzlinger, G. Ward, L. Whitehead, M. Trentacoste, A. Ghosh, and A. Vorozcovs, "High dynamic range display systems," *ACM Trans. Graph.* **23**(3), 760–768 (2004).
3. Q. Hong, T. X. Wu, X. Zhu, R. Lu, and S. T. Wu, "Extraordinarily high-contrast and wide-view liquid-crystal displays," *Appl. Phys. Lett.* **86**(12), 121107 (2005).
4. H. Chen, R. Zhu, M. C. Li, S. L. Lee, and S. T. Wu, "Pixel-by-pixel local dimming for high-dynamic-range liquid crystal displays," *Opt. Express* **25**(3), 1973–1984 (2017).
5. A. Takeda, S. Kataoka, T. Sasaki, H. Chida, H. Tsuda, K. Ohmuro, T. Sasabayashi, Y. Koike, and K. Okamoto, "A super-high image quality multi-domain vertical alignment LCD by new rubbing-less technology," *SID Symp. Dig. Tech. Papers* **29**(1), 1077–1080 (1998).
6. S. H. Lee, S. L. Lee, and H. Y. Kim, "Electro-optic characteristics and switching principle of a nematic liquid crystal cell controlled by fringe-field switching," *Appl. Phys. Lett.* **73**(20), 2881–2883 (1998).
7. M. Schadt and W. Helfrich, "Voltage-dependent optical activity of a twisted nematic liquid crystal," *Appl. Phys. Lett.* **18**(4), 127–128 (1971).
8. Y. Utsumi, I. Hiyama, Y. Tomioka, K. Kondo, and S. Matsuyama, "Analysis of light leakage caused by color filter between crossed polarizers," *Jpn. J. Appl. Phys.* **46**(3A 3R), 1047–1050 (2007).
9. Y. Utsumi, S. Takeda, I. Hiyama, Y. Tomioka, M. Ishii, and K. Ono, "Light leakage behaviors of homogeneously aligned liquid crystal layers placed between crossed polarizers," *Jpn. J. Appl. Phys.* **47**(4 4R), 2144–2148 (2008).
10. K. Sumiyoshi, "Light leakage analysis of in-plane-switching liquid crystal displays," *Jpn. J. Appl. Phys.* **48**(12 12R), 121601 (2009).
11. M. Ishiguro, M. Sekiguchi, and Y. Saitoh, "New approach to enhance contrast ratio at normal incidence by controlling the retardation of optical compensation film in vertically aligned liquid crystal displays," *Jpn. J. Appl. Phys.* **49**(3 3R), 030208 (2010).
12. H. K. Kim, D. Y. Lee, and J. K. Song, "Contrast ratio of twisted nematic liquid crystal cells and its improvement," *Liq. Cryst.* **38**(10), 1239–1244 (2011).
13. Y. Utsumi, D. Kajita, S. Takeda, H. Kagawa, I. Hiyama, Y. Tomioka, and K. Ono, "Correlation of light scattering of homogenous alignment liquid crystal layers with material properties of liquid crystals," *Jpn. J. Appl. Phys.* **47**(4 4R), 2205–2208 (2008).
14. Y. Utsumi, I. Hiyama, Y. Tomioka, and K. Ono, "Quantitative analysis method for measuring light leakage intensity of three primary color filters placed between crossed polarizers," *Jpn. J. Appl. Phys.* **47**(5 5R), 3518–3521 (2008).
15. J. S. Hsu, Y. H. Lin, H. C. Lin, and K. H. Yang, "Thermally induced light leakage in in-plane-switching liquid crystal displays," *J. Appl. Phys.* **105**(3), 033503 (2009).
16. J. S. Park, "Contrast ratio of colorant film: Theoretical consideration and effect of polymeric binder," *J. Appl. Polym. Sci.* **117**(1), 428–433 (2010).

17. M. Akimoto, J. Iwakawa, N. Kobayashi, S. Kobayashi, and K. Takatoh, "Evaluation of liquid crystal alignment ability of polyimide by analyzing the black state of homogeneous alignment liquid crystal display," *Mol. Cryst. Liq. Cryst.* **543**(1), 69–835 (2011).
18. H. Takemoto, T. Fuchida, and M. Miyatake, "Analysis of depolarized light-scattering in LCD panel and proposal of LCD systems for enhancing contrast ratio," *SID Symp. Dig. Tech. Papers* **40**(1), 514–517 (2009).
19. Y. Utsumi, S. Takeda, H. Kagawa, D. Kajita, I. Hiyama, Y. Tomioka, T. Asakura, M. Shimura, M. Ishii, K. Miyazaki, and K. Ono, "Improved contrast ratio in IPS-Pro LCD TV by using quantitative analysis of depolarized light leakage from component materials," *SID Symp. Dig. Tech. Papers* **39**(1), 129–132 (2008).
20. K. J. Kim, T. R. Lee, H. H. Son, D. K. Kim, J. H. Baek, J. H. Kim, and M. Jun, "Realization of true black quality in in-plane switching mode for LCD TV applications," *SID Symp. Dig. Tech. Papers* **41**(1), 487–490 (2010).
21. K. Okumoto, T. Tsuchiya, K. Yonemura, S. Nagano, O. Tanina, A. Yuuki, T. Fujino, and T. Satake, "A novel simulation method in in-plane switching mode panel with considering light scattering behavior," *SID Symp. Dig. Tech. Papers* **46**(1), 1555–1558 (2015).
22. M. Yoneya, Y. Utsumi, and Y. Umeda, "Depolarized light scattering from liquid crystals as a factor for black level light leakage in liquid-crystal displays," *J. Appl. Phys.* **98**(1), 016106 (2005).
23. R. Lu, Q. Hong, S. T. Wu, K. H. Peng, and H. S. Hsieh, "Quantitative comparison of color performances between IPS and MVA LCDs," *J. Disp. Technol.* **2**(4), 319–326 (2006).
24. H. Chen, F. Peng, Z. Luo, D. Xu, S. T. Wu, M. C. Li, S. L. Lee, and W. C. Tsai, "High performance liquid crystal displays with a low dielectric constant material," *Opt. Mater. Express* **4**(11), 2262–2273 (2014).
25. Z. Ge, X. Zhu, T. X. Wu, and S. T. Wu, "High transmittance in-plane-switching liquid crystal displays," *J. Disp. Technol.* **2**(2), 114–120 (2006).
26. Y. Ukai, T. Ohyama, L. Fennell, Y. Kato, M. Paukshto, P. Smith, O. Yamashita, and S. Nakanishi, "Current status and future prospect of in-cell-polarizer technology," *J. Soc. Inf. Disp.* **13**(1), 17–24 (2005).
27. S. H. Kim, J. D. Park, and K. D. Lee, "Fabrication of a nano-wire grid polarizer for brightness enhancement in liquid crystal display," *Nanotechnology* **17**(17), 4436–4438 (2006).
28. Z. Ge and S. T. Wu, "Nanowire grid polarizer for energy efficient and wide-view liquid crystal displays," *Appl. Phys. Lett.* **93**(12), 121104 (2008).
29. F. Yamada, H. Nakamura, Y. Sakaguchi, and Y. Taira, "Sequential-color LCD based on OCB with an LED backlight," *J. Soc. Inf. Disp.* **10**(1), 81–85 (2002).
30. F. C. Lin, Y. P. Huang, C. M. Wei, and H. P. D. Shieh, "Color-breakup suppression and low-power consumption by using the Stencil-FSC method in field-sequential LCDs," *J. Soc. Inf. Disp.* **17**(3), 221–228 (2009).

1. Introduction

High contrast ratio (CR) is a critical requirement for all the display devices, as it affects the perceived image quality [1–4]. For a non-emissive liquid crystal display (LCD), its CR depends on the liquid crystal (LC) modes and is inherently limited. For examples, the typical CR for commercial vertical-alignment (VA) LCD TVs is about ~5000:1 [5], but drops to ~2000:1 for the fringe-field switching (FFS)-based LCD smartphones and tablets [6], and then ~1000:1 for twisted nematic (TN)-based notebook and desktop computers [7]. To improve CR, increasing the polarizer thickness is a straightforward approach. However, more evidences reveal that polarizer is no longer the limiting factor [8–12]. In fact, it is fairly easy to get $CR > 100,000:1$ with two high-quality crossed polarizers, but the final CR of an LCD is still limited to 5,000:1, which is mainly governed by the depolarization effect inside the LCD panel. The origins for this depolarization are rather complicated, including diffraction effect, scattering effect, misalignment effect, etc [13–18]. After extensive studies, the underlying physical mechanisms have been gradually understood, and their contributions to the total depolarization can be evaluated quantitatively [19, 20], as will be discussed later.

Although the depolarization effect has been verified experimentally and investigated systematically, how to incorporate this effect into the simulation model remains to be a big challenge [21]. Actually, for the commercial software DIMOS or TechWiz, this depolarization effect is completely neglected, and the calculated CR is solely determined by the polarizers without considering the depolarization or scattering effect. Therefore, it is quite common to obtain $CR > 10,000:1$ in simulations, but in reality it is much lower. If the CR is not accurate, let alone the viewing angle. Therefore, there is urgent need to build a more rigorous model taking the depolarization effect into consideration, which helps not only understand the underlying physical mechanisms but also guide the device and material optimizations.

In this paper, we build a physical model by introducing a depolarization coefficient (A). With that, we could accurately simulate the contrast ratio and viewing angle. Also, based on this model, we propose a new device structure to mitigate the depolarization effect, leading to a much improved CR. Other possible approaches to enlarge CR are also discussed.

2. New simulation model

2.1 Polarizer effect

Before introducing the new simulation model, firstly we have to know how the conventional model works. Here, we choose a commercial software TechWiz (Sanayi, Korea) as an example. In our simulation, the parameters for polarizer and analyzer are: $n_o = 1.5$, $k_o = 0.000306$, $n_e = 1.5$, and $k_e = 0.019027$. As usual, n_o (k_o) and n_e (k_e) represent the real (imaginary) part of ordinary and extraordinary refractive index, respectively. Then, polarizer (analyzer) thickness is varied from 15 μm to 30 μm , and the obtained results are shown in Fig. 1. As expected, when the thickness of polarizer (or analyzer) increases, the transmittance of both bright state and dark state decreases, but at different rates [Fig. 1(a)]. As a result, the corresponding CR increases exponentially [Fig. 1(b)], and CR > 100,000:1 can be realized by simply increasing the polarizer thickness to over 29 μm . However, this is only for the ideal case. In reality, due to the depolarization effect of LCD components, the CR is limited to $\sim 5000:1$ for VA mode and $\sim 2000:1$ for FFS mode.

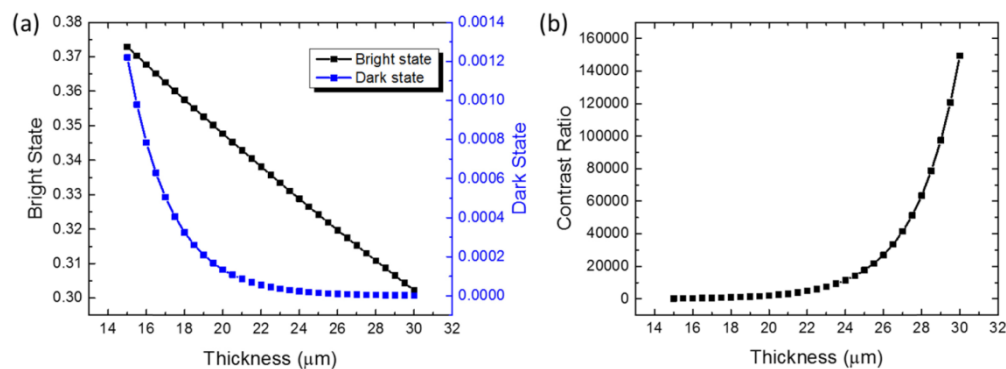


Fig. 1. (a) Simulated transmittance of bright state and dark state, and (b) simulated CR as a function of polarizer thickness. No depolarization effect is considered.

2.2 Depolarization effect

The origins for depolarization are rather complicated; they may come from the diffraction effect of patterned thin-film transistors (TFTs) and electrode, scattering effect from LC layer and color filter (CF) array, misalignment of crossed polarizers, and rubbing scratches, etc [8, 14–20]. Figure 2 schematically depicts some of them. Moreover, these physical origins make different contributions for different LC modes. For example, in FFS and in-plane switching (IPS) modes, scattering effect from LC director's thermal fluctuation contributes 50%-60% to the total depolarization effect (also known as degree of imperfection), while CF pigment scattering makes 30%-40% [19, 20]. But in VA mode, LC scattering is greatly reduced, thus CF scattering turns out to be the dominant factor [22].

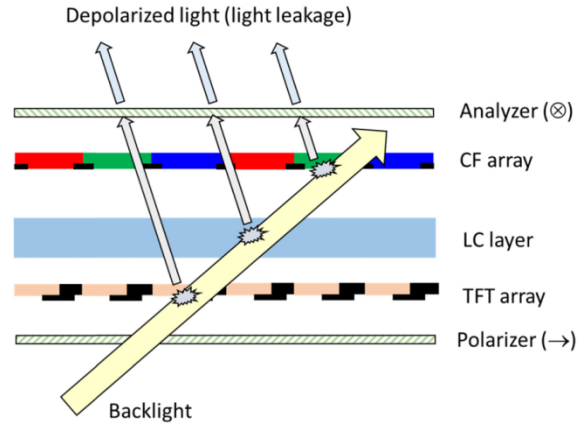


Fig. 2. Schematic diagram for accounting the depolarization effect in an LCD panel. CF: color filter; LC: liquid crystal; TFT: thin-film transistor.

2.3 Depolarization coefficient (A)

Next, to quantify the depolarization effect we introduce a depolarization coefficient (A), which is described by:

$$I'_x = I_x \cdot (1 - A) + I_y \cdot A, \quad (1)$$

$$I'_y = I_x \cdot A + I_y \cdot (1 - A), \quad (2)$$

where I_x (I_y) and I'_x (I'_y) represent the intensity of original light and scattered light along two orthogonal polarization directions, respectively. In theory, each depolarization mechanism should have one coefficient, like A_1 for electrode diffraction, A_2 for LC scattering, A_3 for CF scattering, etc. But for simplicity we can define an *effective* depolarization coefficient (A_{eff}), which is the sum of each individual coefficient:

$$A_{eff} = A_1 + A_2 + A_3 + \dots \quad (3)$$

This could be illustrated as follows. Let us start from the simplest case: A_1 and A_2 . They are governed by these equations:

$$\begin{aligned} I'_{1x} &= I_{1x} \cdot (1 - A_1) + I_{1y} \cdot A_1 \\ I'_{1y} &= I_{1x} \cdot A_1 + I_{1y} \cdot (1 - A_1) \\ I'_{2x} &= I'_{1x} \cdot (1 - A_2) + I'_{1y} \cdot A_2 \\ I'_{2y} &= I'_{1x} \cdot A_2 + I'_{1y} \cdot (1 - A_2) \end{aligned} \quad (4)$$

With simple algebra, we obtain:

$$\begin{aligned} I'_{2x} &= I_{1x} \cdot [1 - (A_1 + A_2) + 2A_1A_2] + I_{1y} \cdot [(A_1 + A_2) - 2A_1A_2], \\ I'_{2y} &= I_{1x} \cdot [(A_1 + A_2) - 2A_1A_2] + I_{1y} \cdot [1 - (A_1 + A_2) + 2A_1A_2]. \end{aligned} \quad (5)$$

In practice, A_1 and A_2 are relatively small and we can neglect the higher order term $2A_1A_2$. Under such condition, Eq. (5) is simplified to:

$$\begin{aligned} I'_{2x} &\approx I_{1x} \cdot (1 - A_{eff}) + I_{1y} \cdot A_{eff}, \\ I'_{2y} &\approx I_{1x} \cdot A_{eff} + I_{1y} \cdot (1 - A_{eff}). \end{aligned} \quad (6)$$

In Eq. (6), $A_{eff} = A_1 + A_2$. Similarly, although multiple depolarization factors could coexist in an LCD panel, we could treat them as a single coefficient A in the simulation.

3. Simulation results

With the introduction of depolarization coefficient A , now we can perform the calculations. Figure 3 depicts the flow chart of our new simulation model. Compared to the conventional one, the only difference is the introduction of a scattering module. Next, to illustrate the effectiveness of our new model, we choose MVA and FFS as two examples.

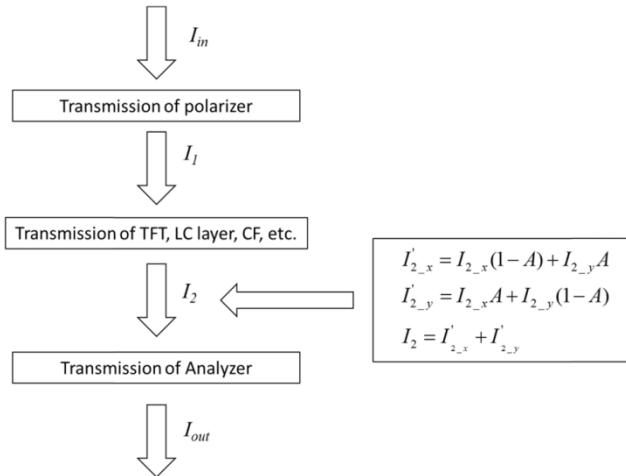


Fig. 3. Flow chart of the proposed simulation model.

3.1 Simulated contrast ratio

a) MVA mode

Due to the fast response time and high contrast ratio, MVA has been widely used in large-sized TVs [1, 5]. Here, we choose it as an example to elucidate the simulation procedures. The employed LC mixture and electrode structure are the same as those reported in [23]: MLC-6608 (Merck), electrode width $w = 6 \mu\text{m}$, electrode gap $g = 42 \mu\text{m}$, and cell gap $d = 4 \mu\text{m}$. Compensation films are implemented to suppress the color shift and gamma shift at large oblique angles. Polarizer and analyzer are $24\text{-}\mu\text{m}$ thick with $n_o = 1.5$, $k_o = 0.000306$, $n_e = 1.5$, and $k_e = 0.019027$. Unless otherwise stated, all the contrast ratios presented here are evaluated at $\lambda = 550 \text{ nm}$.

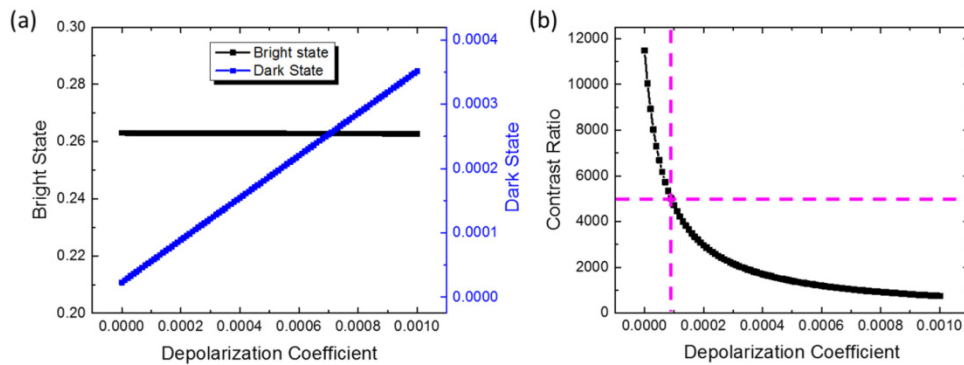


Fig. 4. (a) Simulated transmittance of bright state and dark state, and (b) simulated CR as a function of depolarization coefficient for MVA mode. Depolarization effect is considered.

With all other parameters being known, the depolarization coefficient A can be extracted easily from the measured contrast ratio. Figure 4(a) shows the transmittance of bright state and dark state as a function of A , where bright state is not affected but dark state is degraded significantly as A increases. Figure 4(b) shows the corresponding CR. When $A = 0$ (ideal case without depolarization effect), CR is $\sim 12,000:1$. As A increases (real case with strong depolarization effect), CR decreases almost exponentially. According to the measured result, MVA shows CR $\approx 5000:1$. Thus, from Fig. 4(b) we find $A \sim 0.00009$ for the MVA mode.

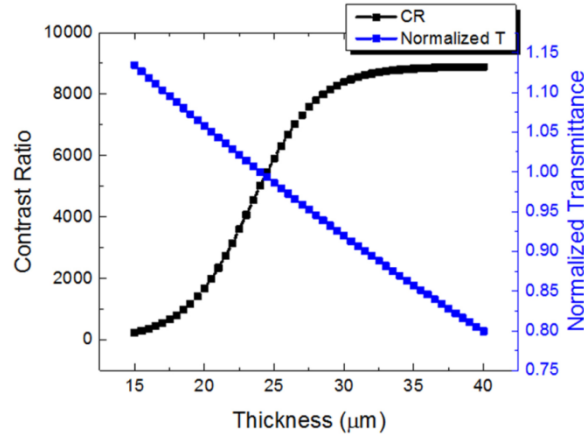


Fig. 5. Simulated contrast ratio and normalized transmittance for MVA mode with depolarization coefficient $A = 0.00009$. Note: 24- μm thick polarizer is the reference with CR $\approx 5000:1$ and efficiency = 1.

With the obtained coefficient A , we can evaluate the real CR for the MVA mode by varying the polarizer thickness. Results are depicted in Fig. 5. Interestingly, as the polarizer gets thicker, CR increases first but then saturates gradually. This trend is quite different from the result using conventional model [Fig. 1(b)]. It indicates that keeps on increasing the polarizer thickness would eventually reach a theoretical limit (CR_{lim}), which is governed by the depolarization coefficient (A) and peak transmittance (T_p):

$$CR_{\text{lim}} = T_p / A. \quad (7)$$

Based on our new model, we could also perform the optimization for polarizer. For example, in Fig. 5, let us set 24- μm thick polarizer as the reference with CR $\approx 5000:1$ and efficiency = 1. As the polarizer thickness increases, CR increases and then saturates but transmittance keeps decreasing. A good balance occurs at 29 μm , where CR is increased by 60% ($\approx 8000:1$) while the transmittance is reduced by 6.8% (93.2%). For comparison, it is unlikely to do the similar optimization with conventional models because the true CR information is obscured.

b) FFS mode

FFS mode exhibits several outstanding features, such as high transmittance, wide viewing angle, weak color shift, and robust to touch pressure [6, 24]. Both positive (p-FFS) and negative (n-FFS) dielectric anisotropy ($\Delta\epsilon$) LC materials can be used in FFS [25]. Here, we focus on n-FFS with zigzag electrode configuration. The employed LC mixture is ZOC-7003 (JNC, Japan), cell gap is 3.11 μm , electrode width is 2.5 μm , and electrode gap is 3.5 μm . The simulated results are plotted in Fig. 6. Due to stronger scattering effect of the LC layer, FFS exhibits a slightly lower CR ($\approx 2000:1$). The corresponding A for FFS is 0.00039, which is about 4x larger than that of MVA ($A \approx 0.00009$).

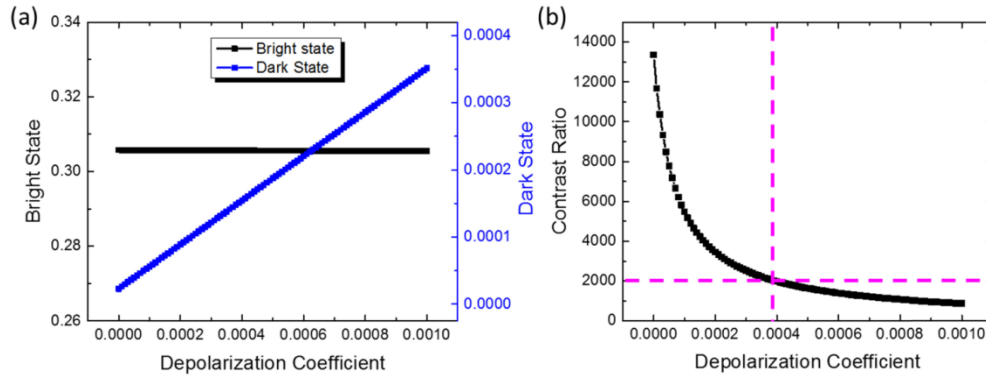


Fig. 6. (a) Simulated transmittance of bright state and dark state, and (b) simulated CR as a function of depolarization coefficient for FFS mode, where depolarization effect is considered.

Figure 7 shows how the polarizer thickness affects the CR and optical efficiency of FFS mode. A similar trend, where CR saturates at 2400:1, is observed. However as the polarizer thickness increases from 24 μm to 29 μm , the CR only improves by 15% (from 2000:1 to 2300:1), which is much less significant than that of MVA mode (15% vs. 60%).

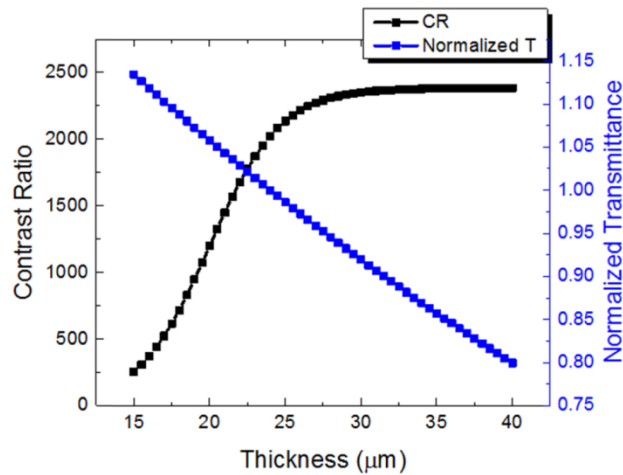


Fig. 7. Simulated contrast ratio and normalized transmittance for FFS mode with depolarization coefficient $A = 0.00039$. Note: 24- μm thick polarizer is the reference for $CR \approx 2000:1$ and efficiency = 1.

c) CR improvement

As discussed above, FFS shows less CR improvement when increasing the polarizer thickness. This can be further investigated by varying the depolarization coefficient, and results are plotted in Fig. 8. As A increases, the CR improvement ($CR_{T=29\mu\text{m}} / CR_{T=24\mu\text{m}}$) gradually saturates. This trend is quite reasonable because CR is jointly determined by the polarizer and the depolarization effect. If depolarization is weaker (smaller A), then the polarizer would make a larger impact, just like MVA mode. On the other hand, if depolarization is strong (large A), then the CR would not be affected too much by the polarizer. Thus, to improve CR of an FFS LCD, the most effective approach is to reduce A rather than increasing the polarizer's thickness. To do so, several methods can be considered, such as optimizing LC alignment [17], choosing a proper LC mixture [9], and reducing the CF pigment size [8].

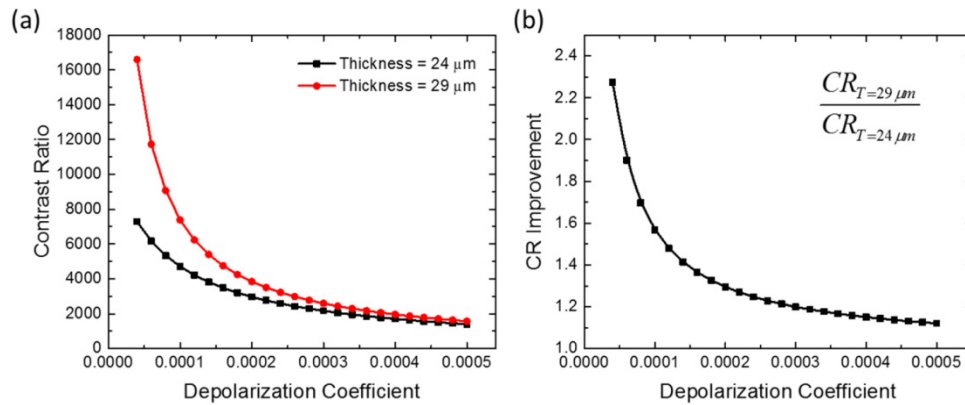


Fig. 8. (a) Simulated contrast ratio and (b) contrast ratio improvement as a function of depolarization coefficient.

3.2 Viewing angle

So far, we only concentrate on the CR at normal angle. Next, we examine the CR at different viewing angles. Please note that, here for simplicity, we assume the depolarization coefficient is constant for the entire viewing zone. In practice, we have to extract these coefficients at each viewing angle, using the method illustrated in Fig. 4(b) and Fig. 6(b). However, as will be discussed later, at large oblique angles, CR is much lower. In that case, depolarization coefficient will not make too much impact.

a) MVA mode

Figure 9 shows the simulated isocontrast contours for the MVA mode. Without considering the scattering or depolarization effect [Fig. 9(a)], the maximum CR obtained by TechWiz is 11,437:1. But when A (≈ 0.00009) is introduced using our new model [Fig. 9(b)], this value is reduced to $CR_{max} = 5011:1$. Clearly, our result is more realistic and representative for practical products. Also, by comparing these two figures we can find a very interesting phenomenon: the high CR region ($> 4000:1$) shrinks noticeably, while the low CR region ($< 500:1$) remains almost the same. This finding is consistent with our previous result shown in Fig. 8, which indicates higher CR is more sensitive to the depolarization effect.

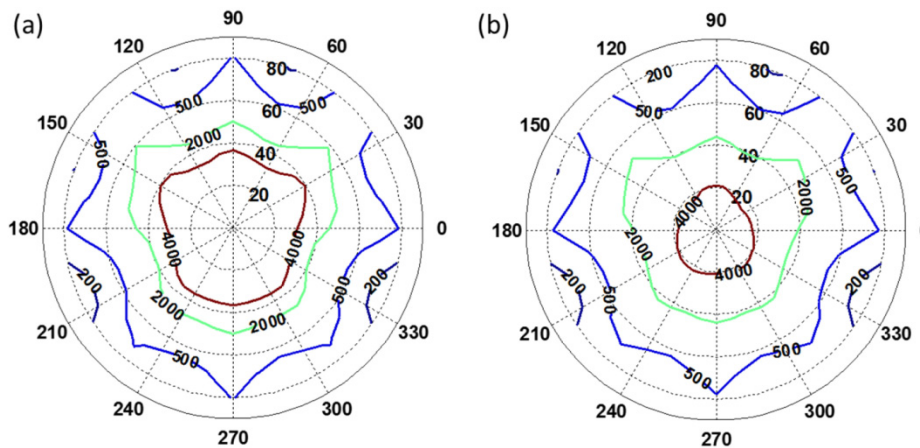


Fig. 9. Simulated isocontrast contour for (a) ideal MVA mode using TechWiz, where $CR_{max} = 11,437:1$, $CR_{min} = 132:1$, and $CR_{ave} = 4350:1$. (b) Real MVA with $A=0.00009$, where $CR_{max} = 5011:1$, $CR_{min} = 130:1$, and $CR_{ave} = 2392:1$. For both cases, the polarizer thickness is 24 μm.

Now the maximum CR is about 5000:1. To enlarge this value, we could increase the polarizer thickness from 24 μm to 29 μm , as described above. The obtained CR_{max} is 8000:1, and meanwhile the viewing angle is widened, especially in the central part [Fig. 10(a)]. If we can further reduce the depolarization coefficient by 20% (from 0.00009 to 0.000071 using the methods mentioned above), then the maximum CR would increase to 10,066:1 [Fig. 10(b)].

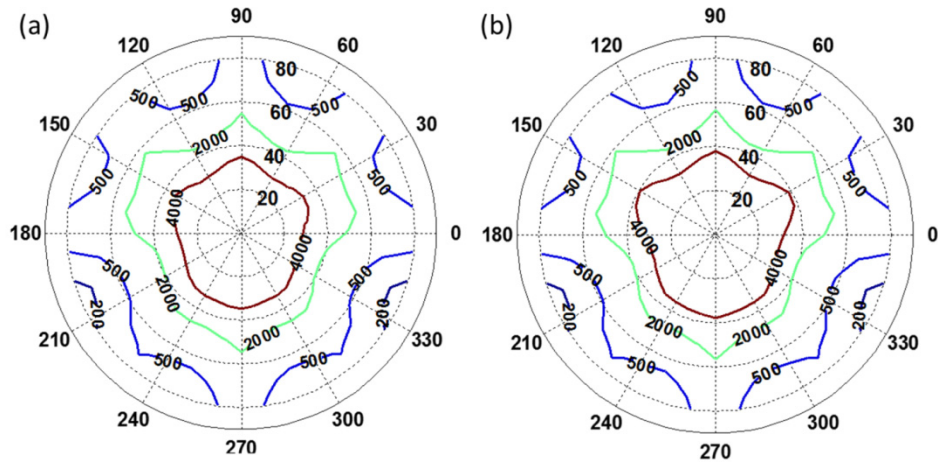


Fig. 10. Simulated isocontrast contour for (a) a realistic MVA with polarizer thickness = 29 μm and $A = 0.00009$, where $CR_{max} = 8129:1$, $CR_{min} = 147:1$, and $CR_{ave} = 3501:1$. (b) Same MVA but with polarizer thickness = 29 μm and $A = 0.000071$, where $CR_{max} = 10,066:1$, $CR_{min} = 148:1$, and $CR_{ave} = 4077:1$.

b) FFS mode

Next, we examine the viewing angle property of FFS mode, and results are shown in Fig. 11. A big difference is observed between conventional model (ideal case) and our new model with depolarization coefficient $A = 0.00039$. For example, in Fig. 11(a), the maximum CR is as high as 13,150:1, and $CR > 5000:1$ covers a large region. But using our new model [Fig. 11(b)], CR_{max} is only 2024:1, and the contrast ratio in the central viewing zone is reduced to 1500:1, which is more consistent to the measured results.

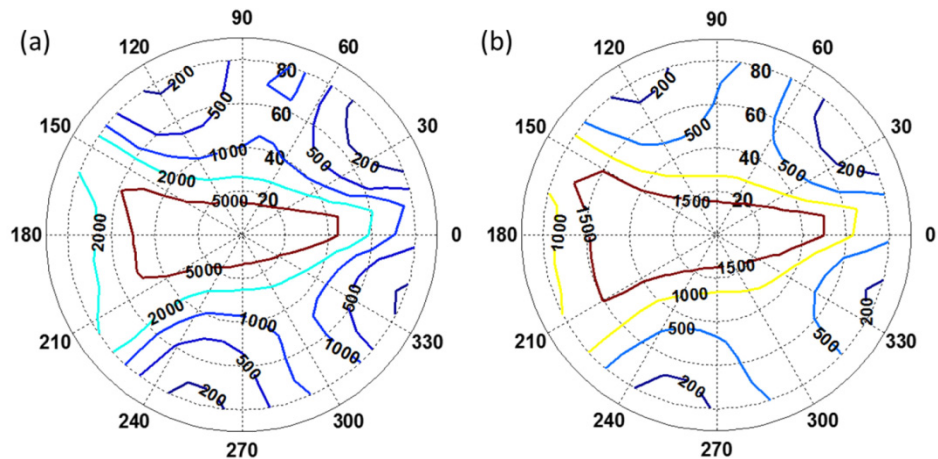


Fig. 11. Simulated isocontrast contour for (a) an ideal FFS mode using TechWiz, where $CR_{max} = 13,150:1$, $CR_{min} = 105:1$, and $CR_{ave} = 4467:1$. (b) A realistic FFS with depolarization coefficient $A = 0.00039$, where $CR_{max} = 2024:1$, $CR_{min} = 100:1$, and $CR_{ave} = 1184:1$. For both cases, the polarizer thickness is 24 μm .

4. New device configuration

4.1 Device structure

As aforementioned, depolarization (scattering) coefficient A plays a key role for improving the contrast ratio and viewing angle. To reduce A , here we propose a new device structure, as Fig. 12 depicts, by adding an in-cell polarizer between the LC layer and the color filters [26]. The remaining structure remains the same as conventional LCD panel. Please note that the transmission axis of in-cell polarizer is parallel to that of analyzer. Because of the introduction of in-cell polarizer, the depolarization coefficients for each layer are decoupled. That is to say, below the in-cell polarizer, depolarization is mainly from TFT substrate and LC layer, which is marked as A_1 ; while above the in-cell polarizer, depolarization is mainly governed by the scattering effect of color filter pigment, marked as A_2 . Then A_1 and A_2 should be treated separately, as will be discussed later.

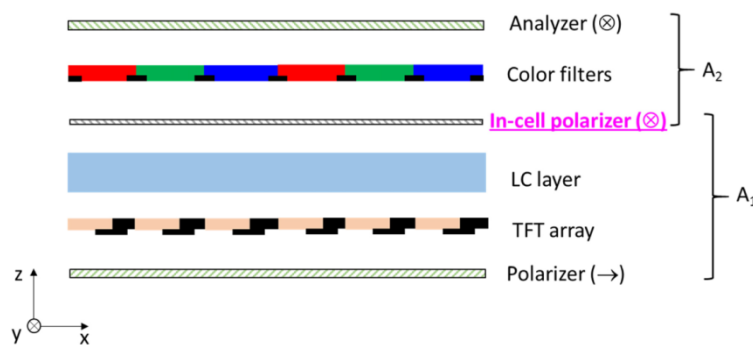


Fig. 12. Schematic diagram of the proposed device structure with an in-cell polarizer.

4.2 Operation principles

Figures 13(a) and 13(b) show the detailed working mechanism. For conventional one [Fig. 13(a)], when backlight goes through the front polarizer, it becomes linearly polarized, say along x-axis. Then after passing through the TFT substrate and LC layer, there is some light leakage along y-axis due to scattering effect. Here, it is governed by A_1 . After the light passing through color filters, the depolarization becomes more severe, represented by $A_1 + A_2$. When entering the analyzer, the x-polarized (dominant polarization direction) light is blocked as expected, while only the depolarized light (jointly determined by $A_1 + A_2$) could traverse through the analyzer. This undesirable light leakage degrades the contrast ratio [19, 20].

For our proposed device structure [Fig. 13(b)], the depolarization effect remains the same for the TFT substrate and LC layer, which is A_1 . But above the LC layer, there is an in-cell polarizer to absorb the x-polarized light; only the scattered light could leak through and enter the color filter array (although it has strong scattering effect). In this case, the depolarized light is still governed by A_1 , and it becomes the final light leakage. Therefore, the effective CR would be enhanced greatly.

Another important point should be mentioned here is that the extinction ratio of in-cell polarizer is not too critical. As long as most of the x-polarized light (dominant polarization direction) is absorbed by the in-cell polarizer, the whole system should work equally well. In that way, high transmittance would be realized. In fact, in our simulation as will be shown later, a 1- μm -thick lyotropic LC-based in-cell polarizer is employed. Its extinction ratio is only $\sim 2000:1$. Even if this in-cell polarizer has an extinction ratio as low as $100:1$, according to our analysis, the final CR performance would not degrade too much, because only 1% of the leaked light would be scattered by the CF pigments. As a result, the final light leakage remains negligible for the MVA and FFS mode.

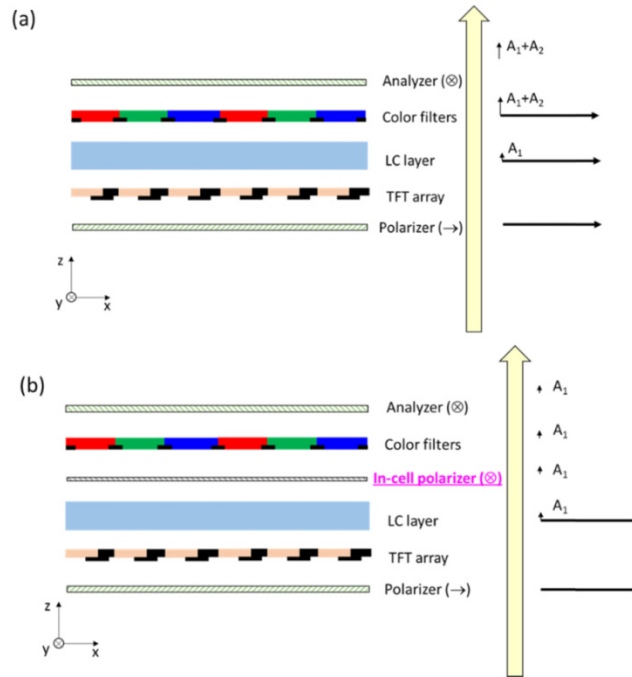


Fig. 13. Working mechanism of (a) conventional LCD panel with depolarization effects, and (b) the proposed LCD panel with decoupled depolarization effects.

4.3 Simulation results

In our simulation, we assume the in-cell polarizer is 1- μm thick with $n_o = 1.5$, $k_o = 0.0003$, $n_e = 1.5$, and $k_e = 0.364$. Since the depolarization coefficients are decoupled intentionally, the calculation flow chart would be slightly different from previous one, as shown in Fig. 14.

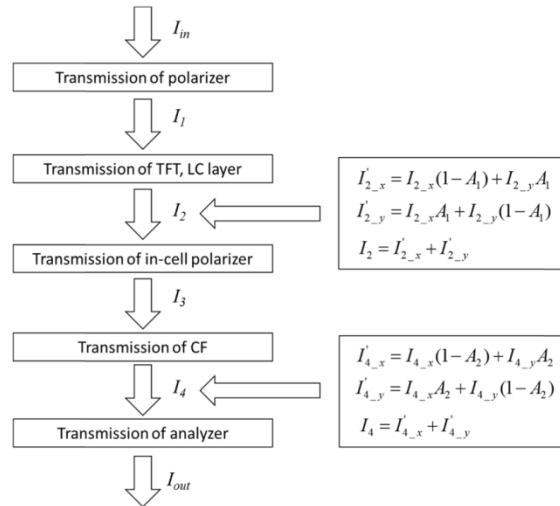


Fig. 14. Flow chart of the proposed simulation model for new structure configuration.

a) MVA mode

According to the analyses from both experiment [15] and simulation [22], LC scattering in MVA mode is more forgiven than that in FFS mode due to their different alignment

directions (homeotropic vs. homogeneous). Therefore, in MVA calculations, we set $A_1 = 0.00003$ and $A_2 = 0.00006$ ($A_1 < A_2$); while in FFS mode it is reversed, i.e. $A_1 > A_2$, as will be discussed later. Figure 15 shows the simulated viewing angle of new MVA mode. For conventional 24 μm thick polarizer [Fig. 15(a)], the maximum CR is improved to 12,277:1, which is about 2.4x higher than that of conventional one shown in Fig. 9(b). Also, the high CR region is greatly widened, and the average CR for entire viewing zone is $> 4,500:1$. If we slightly increase the polarizer thickness to 29 μm [Fig. 15(b)], the maximum CR is improved to 23,163:1. This is a record-high CR for LCD. Please note that all these results are realized using our new model which includes the depolarization effect.

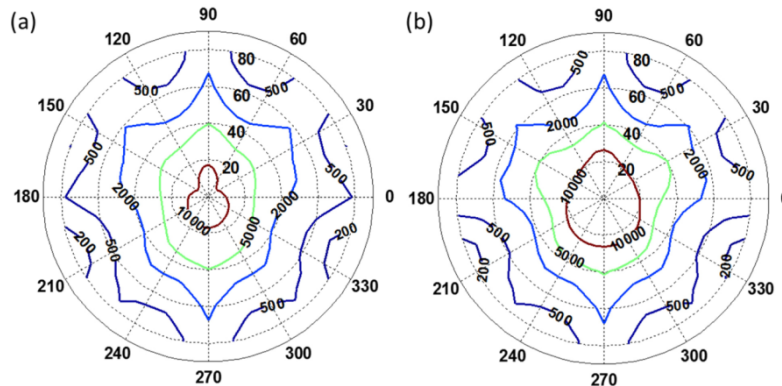


Fig. 15. Simulated isocontrast contour for the proposed device configuration in MVA mode. (a) Polarizer thickness is 24 μm , and (b) polarizer thickness is 29 μm . For the 24- μm thick polarizer: $CR_{max} = 12,277:1$, $CR_{min} = 132:1$, and $CR_{ave} = 4685:1$. For the 29- μm thick polarizer: $CR_{max} = 23,163:1$, $CR_{min} = 149:1$, and $CR_{ave} = 7223:1$.

b) FFS mode

Figure 16 depicts the isocontrast contour of the new FFS mode with an in-cell polarizer. Here, we set $A_1 = 0.00026$ and $A_2 = 0.00013$, since the light leakage mainly originates from LC scattering [19, 20]. From Fig. 16(a), the maximum CR is improved to 3000:1, which is higher than the theoretical limit of 2400:1 shown in Fig. 7. Similarly, increasing the polarizer thickness to 29 μm [Fig. 16(b)] would further boost the CR_{max} to 3349:1. And $CR > 3000:1$ is extended to $\pm 60^\circ$ in the horizontal viewing direction.

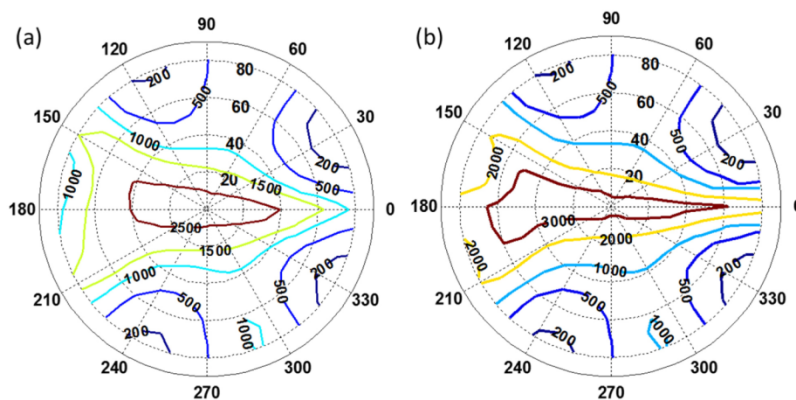


Fig. 16. Simulated isocontrast contour for the new FFS with an in-cell polarizer. (a) Polarizer thickness is 24 μm , and (b) polarizer thickness is 29 μm . For the 24- μm thick polarizer: $CR_{max} = 3002:1$, $CR_{min} = 115:1$, and $CR_{ave} = 1576:1$. For the 29- μm thick polarizer: $CR_{max} = 3349:1$, $CR_{min} = 115:1$, and $CR_{ave} = 1819:1$.

5. Discussion

So far, high CR ($> 10,000:1$) has been realized by adding an in-cell polarizer between LC layer and color filter array to decouple the depolarization effect. Actually, based on the same concept, various device configurations can be considered.

5.1 Dual in-cell polarizers

For practical applications, the in-cell polarizer can be placed in other places to decouple the depolarization coefficient of desired layers. Of course, we could also add more than one in-cell polarizer to the LCD panel to decouple each layer. For example, in Fig. 17 we add two in-cell polarizers on both sides of the LC cell. Under such condition, the depolarization coefficient of TFT and LC layer is decoupled so that the CR can be further enhanced. Besides, if the in-cell polarizer exhibits a high polarization ratio, then the crossed polarizer and analyzer can be removed. The device thickness would be much reduced. It could become a strong contender for flexible displays while keeping a high contrast ratio.

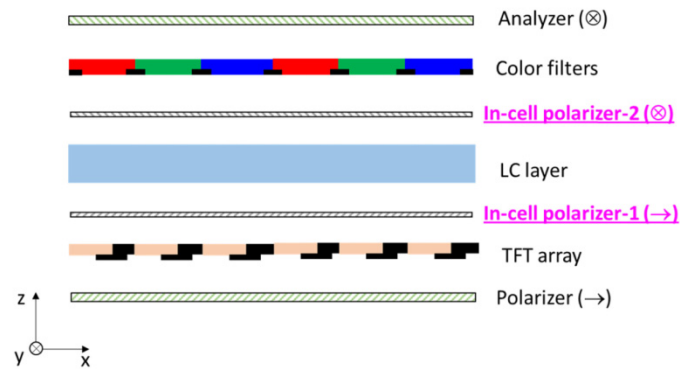


Fig. 17. Schematic diagram of the proposed structure with dual in-cell polarizers. In this case, the polarizer and the analyzer could be removed.

5.2 Reflective polarizer

Figure 18 shows another modification, where in-cell polarizer is replaced by a reflective polarizer, or wire-grid polarizer [27, 28]. In this configuration, the light after LC layer is reflected and recycled, thus higher optical efficiency could be achieved while keeping a high CR. Also, since the transmission axis of this reflective polarizer is parallel to that of analyzer, it will only reflect light from LC side (i.e. backlight side). For ambient light, there is no side effects.

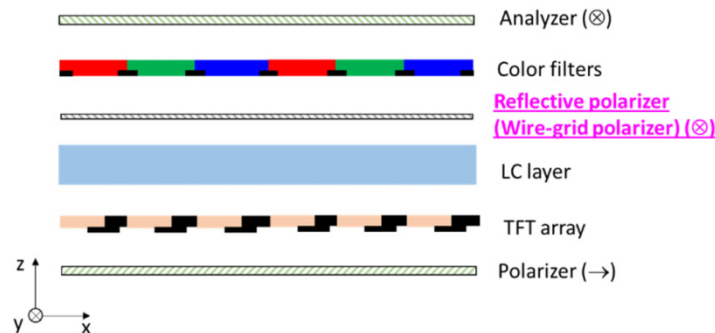


Fig. 18. Schematic diagram of the proposed structure with a reflective polarizer or wire-grid polarizer.

5.3 Field-sequential color display

In a field-sequential color (FSC) display, the color filter array is removed [29, 30]. With a fast-switching LC, both red, green and blue (RGB) sub-frames are obtained in sequential time, as illustrated in Fig. 19, so that both optical efficiency and resolution density are tripled. What's more, based on our analysis, the device contrast ratio could be improved significantly (compared to conventional LCD), because the depolarization effect of color filters is eliminated completely.

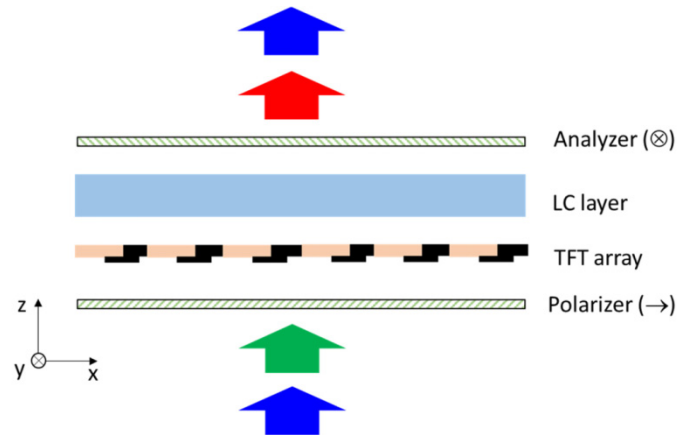


Fig. 19. Schematic diagram of the field-sequential color display.

6. Conclusion

We have built a more rigorous model to simulate an LCD's contrast ratio and viewing angle. It is found that there is an inherent theoretical limit of CR, due to the depolarization effect in TFT substrate, LC layer, CF array, etc. Also, we propose a new device structure, where an additional in-cell polarizer is placed between LC layer and CF array to decouple the depolarization effect. Based on the analysis using our new model, the maximum CR of a MVA LCD could reach over 20,000:1. While for the n-FFS mode, it could reach > 3000:1. Also, we discuss other potential structures to further enhance the CR. We believe our model is a powerful tool to investigate the underlying physical mechanism of CR and guide the future optimizations for LCD devices and materials.

Funding

a.u.Vista, Inc.

Acknowledgment

The authors would like to thank Ruidong Zhu for helpful discussion.